HEPRO VII

HIGH ENERGY PHENOMENA IN RELATIVISTIC OUTFLOWS VII

BARCELONA, 9-12 JULY 2019

FACULTY OF PHYSICS

UNIVERSITY OF BARCELONA

Relativistic Jet of Markarian 421: Observational Evidences of Particle Acceleration Mechanisms

Dr. Associate Prof. Bidzina Kapanadze

E. Kharadze Abastumani Astrophysical Observatory at Ilia State University, Tbilisi, Georgia

INAF, Osservatorio Astronomico di Brera, Italy

In collaboration with Stefano Vercellone and Patrizia Romano (INAF- Brera)

2019 July 10, Barcelona

Mrk 421in Brief

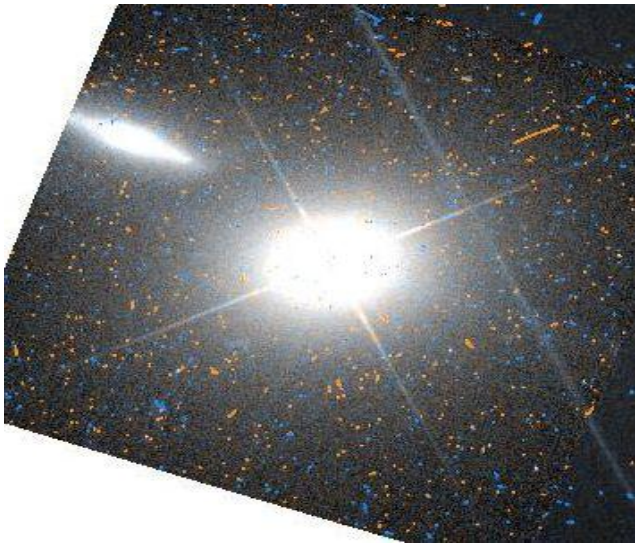

The HST image of Mrk 421
(Scarpa+2000)

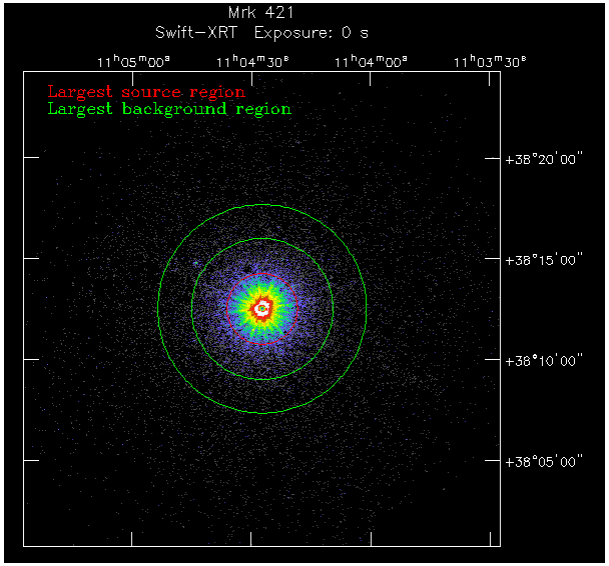

The 0.3-10 KeV image of Mrk 421,
Swift-XRT, PC-mode

- **HBL (BL Lac source with synchrotron SED peak at UV-X-ray frequencies) situated at z=0.031**
- **Active nucleus of bright elliptical galaxy**
- **The first extragalactic TeV source** (Punch +1992) **, and TeV-detected many times afterwards** (Gaidos+1996, Aharonian+1999, 2002, 2003,2005,2007; Acciari+2009,2011,2014; Aielli+2010; Aleksic+2010,2012, 2015a,2015b; Bartoli+2011,2016; Balokovic+2016; Blazejowski+2005; buchley+1996; Charlot+2006; Fossati+2008; Giebels+2007; Kerrick+1995; Konopelko+2008; Krawczynski+2001; Krennrich+1999,2002; Maraschi+1999,; Okomura+2002; Rebillot+2006; Shukla+2012 etc.)
- **Highest-energy photon with E >10 TeV** (Okomura+2002)
- **Extreme VHE flux variability (e.g. flux increase by a factor of >20 in ~30 min** Gaiodos+1996)
- **Bright and violently variable X-ray source: strongest X-ray ourbursts in 2009 June, 2013 April, 2018 January** (Kapanadze+2016,2017,2018a,b, 2019; Balokovic+2016 etc.)
- **Bright optical-UV source and target of the numerous ground-based and space telescopes** (Horan+2009, Carnerero+2017 etc.)
- **Targeted >1100 times with Swift-XRT (including our TOO observations)**

- **Superluminal jet components in some epochs**

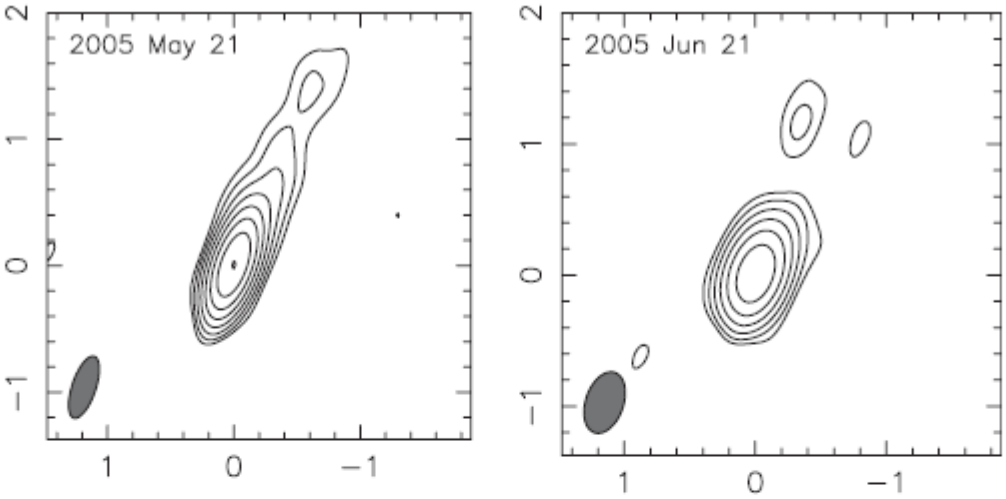

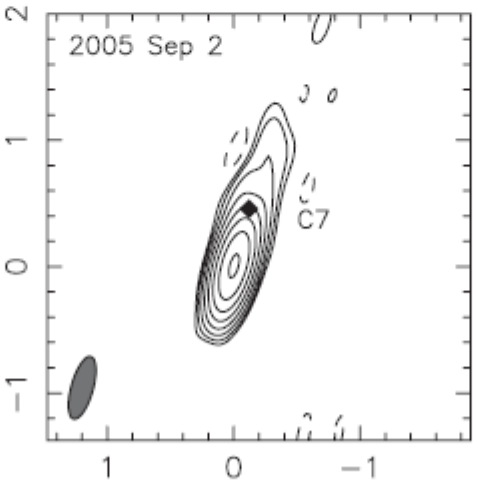

Piner+2010, ApJ, 133, 2357:

Source (1)	Comp. (2)	Upper Limit (c) (3)	r (mas) (4)	r (pc) (5)	r_d (pc) (6)
Mrk 421	C8	2.2	0.23	0.14	3.1

Figure 1. VLBA images of Mrk 421 at 43 GHz during 2005. The axes are labeled in milliarcseconds (mas). The lowest contour is set to three times the rms noise level, and each successive contour is a factor of 2 higher. Numerical parameters of the images are given in Table 1. The position of the center of the circular Gaussian in the inner jet that was fit to the visibilities is marked with a diamond at the last epoch. Parameters of the circular Gaussian models are given in Table 2.

➢ **Non-thermal continuum emission extended from radio to TeV band (17-19 orders of frequency)**

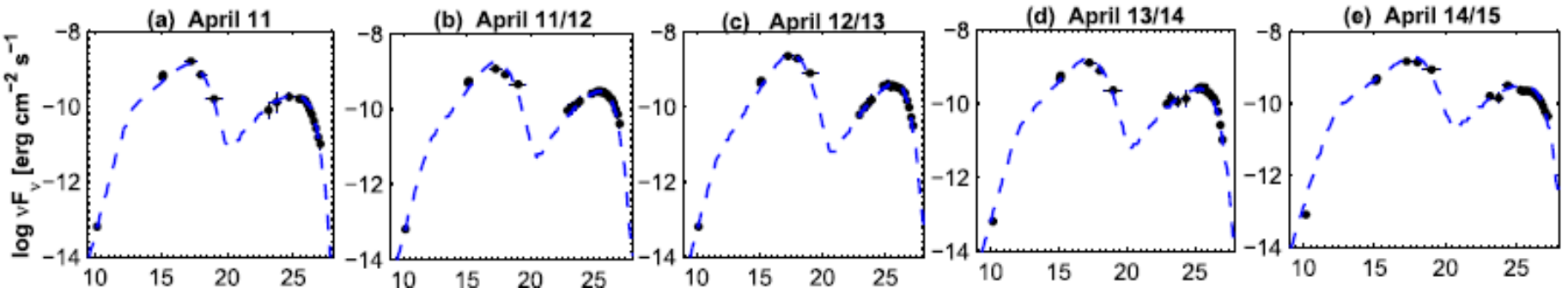

The SED of Mrk 421 during the giant X-ray outburst in 2013 April, one-zone SSC fits (Kapanadze et al. 2016, ApJ, 831, 102).

Quant.	Apr 11	Apr 11/12	Apr 12/13	Apr 13/14	Apr 14/15
$R(10^{16}$ cm)	1.70	1.70	1.70	2.00	2.90
B(Gauss)	0.12	0.10	0.10	0.10	0.07
$N(\mathrm{cm}^{-3})$	2.20	2.10	2.10	2.20	2.20
Γ_L	30	40	40	35	30
δ	30.2	29.0	29.0	29.83	30.2
$\gamma_{min}(\times 10^2)$	5.0	2.8	1.8	2.8	3.5
$\gamma_{max}(\times 10^8)$	1.3	1.8	1.0	1.6	1.6
$\gamma_0(\times 10^4)$	7.0	6.9	7.0	6.0	17.0
r	1.60	1.60	1.40	1.48	1.55
s	2.40	2.10	1.95	2.20	2.40
ν_p^{sync} (10^{17} Hz)	1.49	2.33	3.38	1.41	5.24
ν_p^{SSC} (10^{25} Hz)	1.00	3.92	6.22	2.13	2.72

- **Synchrotron SED peak frequently observed beyond 10 keV during strong X-ray flares**

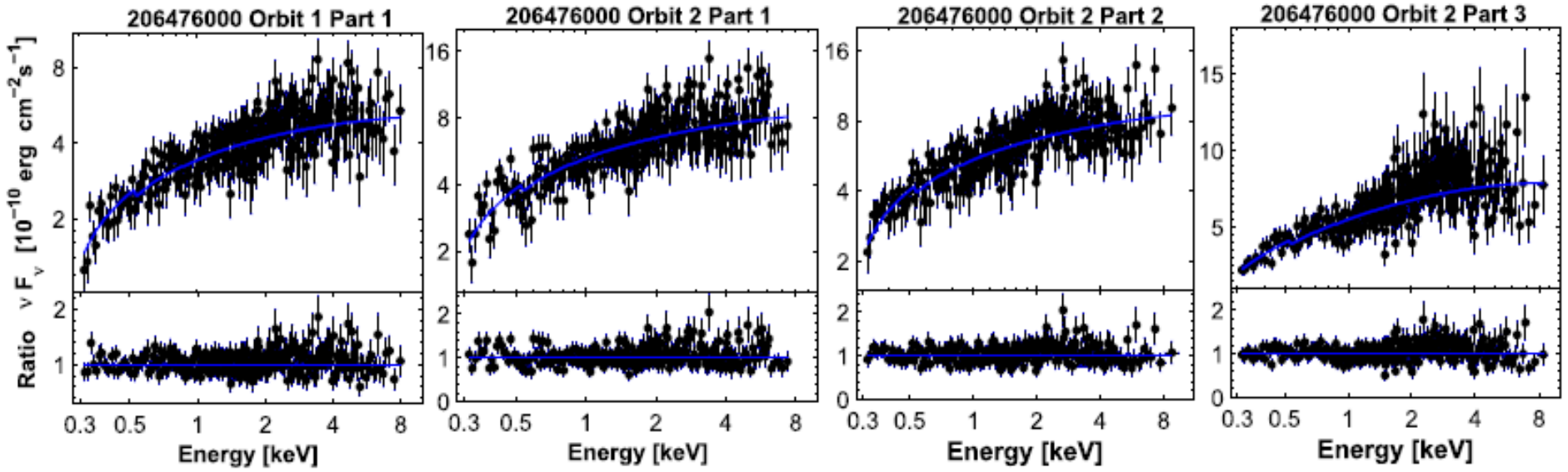

Figure 3. Log-parabolic spectra yielding $E_p > 10$ keV, along with the distribution of the residuals. In each spectrum, a solid line represents the log-normal model

(Kapanadze+2018, ApJ, 854, 66)

Open Problem: Particle Acceleration Processes in the Jet

- **B-Z mechanism** ➔ **The energy stored in rapidly spinning SMBH extracted and channeled into Poynting flux** (Blandford & Znajek 1977, Tchekhovskoy+ 2011) ➔
  - ✓ **Jet power, originally carried by magnetically-dominated beam (with magnetization parameter $\sigma \equiv P_B/P_{kin} >> 1$): progressively used to accelerate matter (≡ conversion from magnetic to kinetic energy), until a substantial equipartition between the magnetic and the kinetic energy fluxes ($\sigma \approx 1$) is established** (Tchekhovskoy +2009)
- **Electrons (+positrons, protons?) should be accelerated to utrarelativistic energies of TeV-order to produce X-ray –HE--VHE photons (via synchrotron and IC mechanisms)**
- **In the bulk frame, for frequencies $\nu \sim 10^{17}$ Hz and B~0.1 G:**
  - ➢ **Radiative lifetimes of electronsh - ~1 hr ➔ minutes in the observer's frame (δ~10)** ➔
  - ➢ **The electron accelerated by BZ-mechanism loose their energy very quickly, emitting X-ray photons (+ IC-scattering)**
  - ➢ **High keV-GeV states, observed on daily-weekly timescales, and X-ray emission detected at sub-pc, pc and sometimes at the kpc distances (Chandra observations; e.g.** Marscher & Jorstad 2011**): <u>some local acceleration mechanisms in BLL jets to be continuously at work</u>**

➢ **Other observational confirmations in favour of "in-situ" re-acceleration:**

- **Significantly higher X-ray luminosity during the flares than the maximal one expected from the initial acceleration**

- **Rapid TeV variability time-scales of a few minutes ➔ shorter, by at least an order of magnitude, than the light-crossing time of the central SMBH with a typical mass ➔**

  ✓ ***V*ariability is associated with small regions of the highly relativistic jet rather than the central region (light-travel argument)**

  ✓ **With the observed t_{var} *and* jet Lorentz factor Γ, the flare should occur at a distance greater than $c\, t_{var}\, \Gamma^2$** (Begelman+2008) **➔ Flaring region situated at *d*> 100r_s from SMBH**

- **The most plausible "in-situ" acceleration mechanisms:**
  - **diffusive shock acceleration (DSA, first-order Fermi mechanism;** Kirk+1998**) at the front of relativistic shocks**
  - **stochastic (second-order Fermi) acceleration by magnetic turbulence (strongly amplified in shocked jet area;** Tramacere+2009**)**
  - **relativistic magnetic reconnection**
  - **shear acceleration**
  - **jet-star interaction**

- **Viability of the first and second-order Fermi mechanisms: presence of X-ray spectral curvature - log-parabolic (LP) spectra emitted by the LP particle energy distribution (PED;** Massaro+2004,2011)

$$F(E)=K(E/E_1)^{-(a+b\log(E/E_1))} \quad ph/cm^2/s$$

with K: normalization factor

E_1: reference energy , fixed to 1 keV

***a*: photon index at 1 keV**

***b*: curvature parameter**

The position of the syncrotron SED peak

$$E_p=E_1 10^{(2-a)/2b} \quad keV$$

Mrk 421, Swift-XRT, obsID 30352115

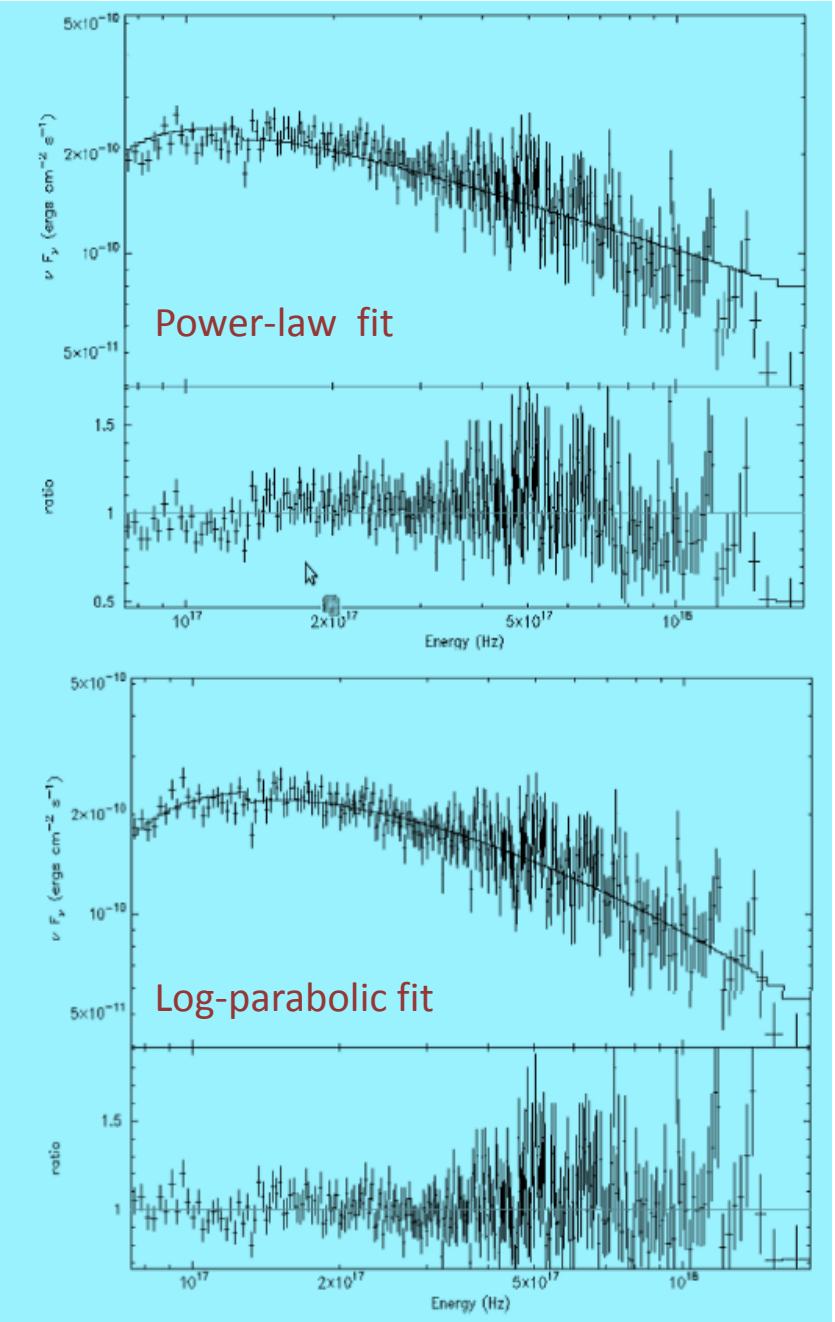

❖ First-Order Fermi Acceleration at Shock Front

- **Statistical acceleration**
- **Relies on repeated scattering of charged particles by magnetic irregularities (Alfven waves; "scattering centres") , confining particles for some time near the shocks**

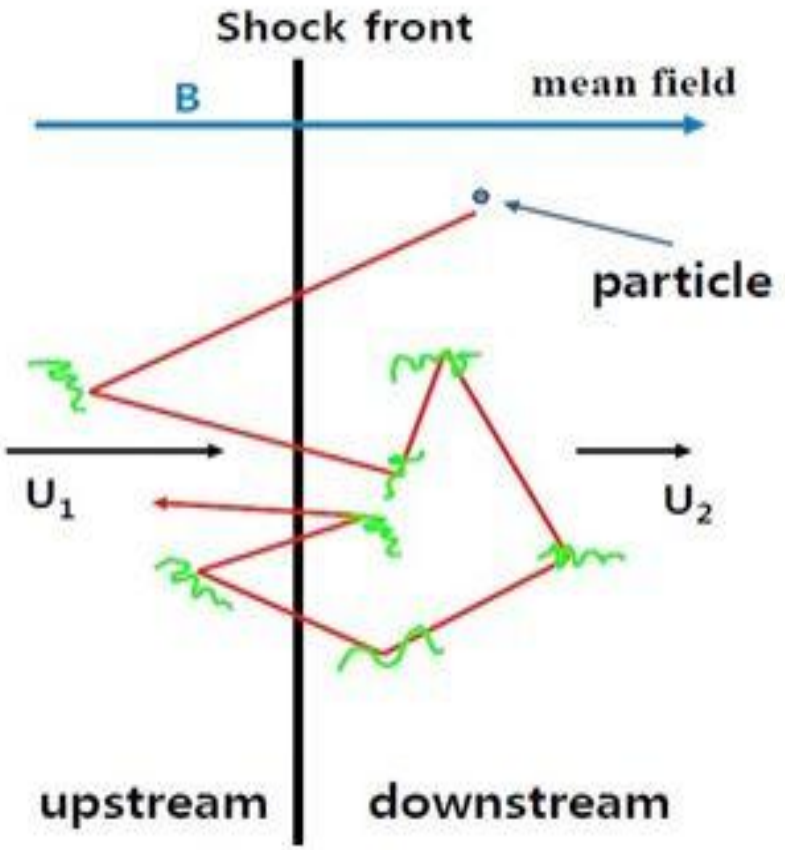

- **Relativistic particle, crossing the shock front , " sees" the scattering centres from the shock upstream and downstream approaching to each other**
- **Energy gain** (Tammi & Duffy 2009)**:**
  - ✓ **by a factor of Γ^2 (with Γ - the bulk Lorentz factor) for the first cycle (crossing the shock front)**
  - ✓ **by a factor of ~2 thereafter**

- **Generally, first-order Fermi mechanism yields a powerlaw spectrum** (Massaro+2004):

$$N(>\gamma) = N_0(\gamma/\gamma_0)^{-s+1}, \quad (10)$$

where $N(>\gamma)$ is the number of particles having a Lorentz factor greater than γ and s is the spectral index given by:

$$s = -\frac{\mathrm{Log}\ p}{\mathrm{Log}\ \varepsilon} + 1, \quad (11)$$

here p is the probability that a particle undergoes an acceleration step i in which it has an energy gain equal to ε, generally assumed both independent of energy:

$$\gamma_i = \varepsilon\gamma_{i-1} \quad (12)$$

and

$$N_i = pN_{i-1} = N_0\, p^i. \quad (13)$$

A log-parabolic energy spectrum follows when the condition that p is independent of energy is released and one assumes that it can be described by a power relation as:

$$p_i = g/\gamma_i^q, \quad (14)$$

where g and q are positive constants; in particular, for $q > 0$ the probability for a particle to be accelerated is lower when its energy increases. Such a situation can occur, for instance, when particles are confined by a magnetic field with a confinement efficiency decreasing for an increasing gyration radius. After

Energy-dependent acceleration probability mechanism (EDAP)

↓

Generation of log-parabolic distribution of particles with energy

- **EDAP prediction: the *a*-*b* correlation**
- **Weak or very weak positive *a*-*b* correlation from the Swift-XRT observations of Mrk 421 during 2005—2018** (Kapanadze 2016a, 2017a, 2018a,b)

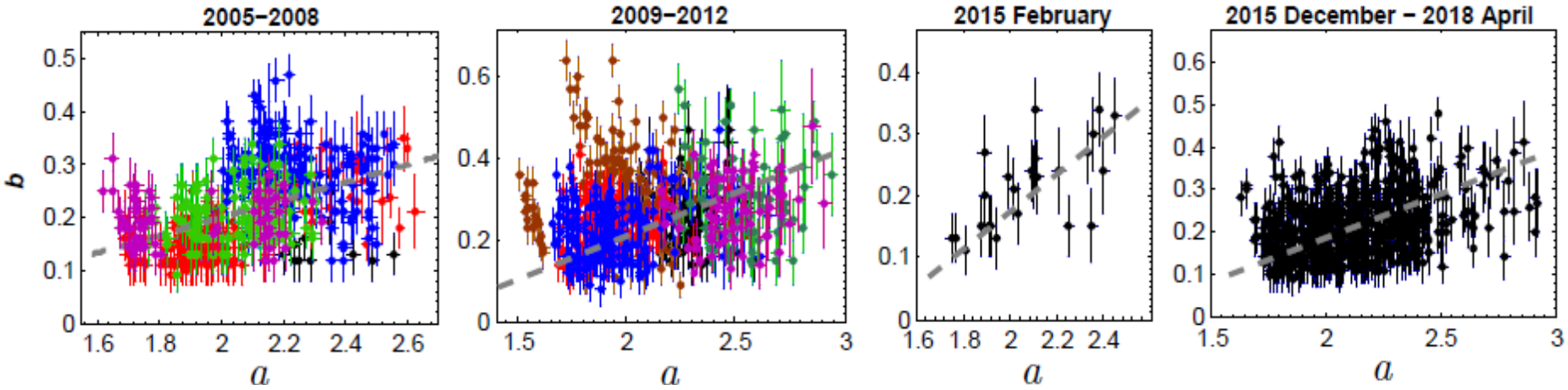

- **"Competition" with other types of the acceleration processes (not yielding such correlation)?**
  - **stochastic**
  - **"classical" first-order Fermi (yielding a powerlaw distribution)**
  - **relativistic reconnection etc.**
- Katarzynski et al. (2006): **charged particle can be accelerated at the shock front by the first-order Fermi process and then continue gaining an additional energy via the stochastic mechanism in the shock downstream region. Eventually, the particle will be able to re-enter the shock acceleration region and repeat the combined acceleration cycle → The a–b correlation will be weak and may not even be observed**

- **Sub-samples with different slopes (corresponding to different periods and underlying physical conditions) in scatter plot - capable to destroy the *a*-*b* correlation in the entire data set even in the case each sub-sample is showing this correlation**
- **Some sub-samples showing even negative the *a*-*b* correlation - expected when $g>\gamma_o$ (i.e. electron population with very low initial energy)**
- **"Competition" with the cooling processes (becoming significant at X-ray frequencies)**

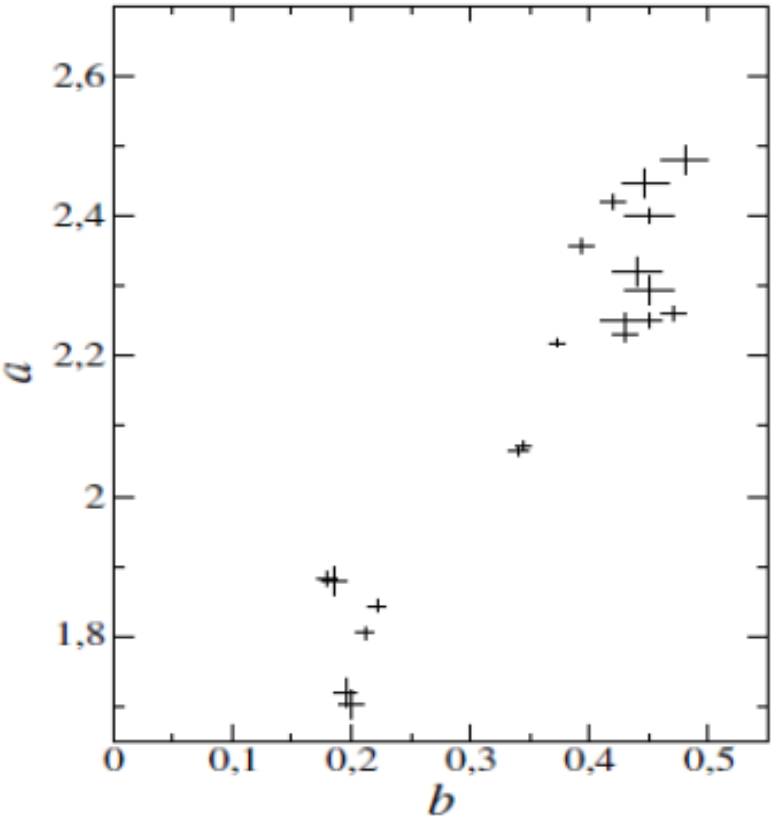

- **Considerably stronger *a*–*b* correlation during the BeppoSAX observations in 1997-1999** (Massaro+2004)

shock. In the Bohm limit, where the particle's mean free path is equal to its gyroradius, $\delta B \sim B$, in which case

$$r_g = \frac{\gamma mc^2}{eB} \approx 1700 \sqrt{\gamma^2 - 1} \left(\frac{B}{1\,\mathrm{G}} \right)^{-1} \ \mathrm{cm}. \quad (1)$$

In this case, the acceleration time-scale can be simplified to

$$\tau_{\mathrm{FI}} \gtrsim 6 \left(\frac{c}{v_s} \right)^2 \frac{\lambda}{c} \approx 6 \frac{r_g c}{v_s^2}, \quad (2)$$

where v_s is the speed of the shock. For a 1-G magnetic field and a relativistic shock ($v_s \to c$), this gives, for an electron with $\gamma = 10^4$, an acceleration time-scale of a few milliseconds. For lower energy particles, the acceleration is even faster. With time resolution of the observations of the order of minutes, this is 'instantaneous'

Tammi & Duffy (2009):

- **EDAP: rapid injection of very energetic particles in the emission zone rather than gradual acceleration** (Cui 2004)
- **Clockwise (CW) spectral evolution in the hardness ratio – flux plane** (Mastichiadis & Moraitis 2008)
- **Observation of the soft lag expected**

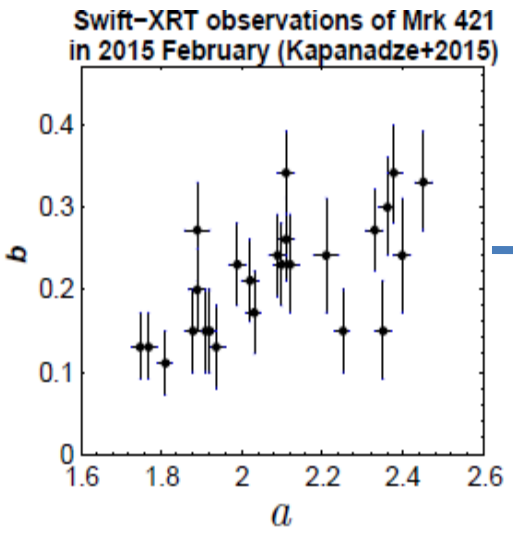

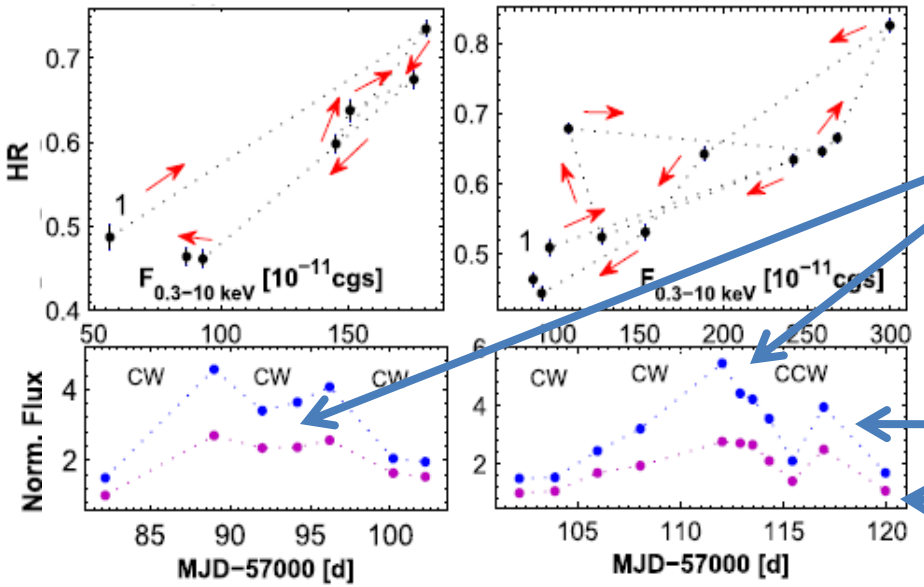

Flux (2-10keV)

Flux (0.3-2keV)

- For protons, however, the mass and acceleration time-scale 1000 times larger than for electrons → No instantaneous injection for the emission zone with significant hadronic contribution
- Similar situation for the electron-positron jet with the magnetic field strength significantly lower than 1 G (e.g. B~0.05 G, often inferred from one-zone SSC modelling) → CCW-type spectral evolution (gradual acceleration) often observed along with the CW-loops in the epochs with the positive a-b correlation

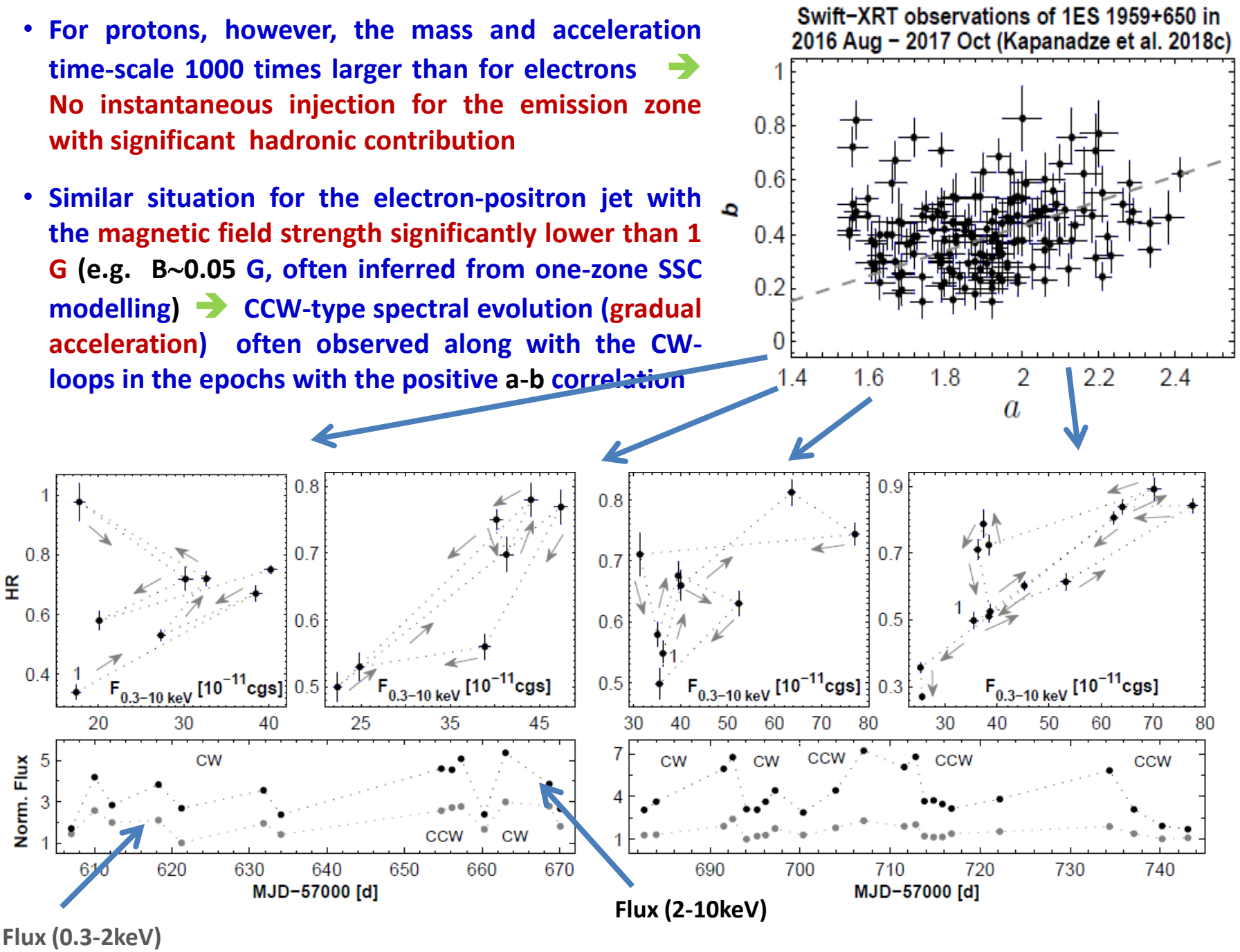

Stochastic Acceleration

- **Operating in the turbulent jet area - accelerating particles using scattering centers moving relative to each other, even without differences in the actual flow speed**
- **Alfven waves in the turbulent downstream of relativistic shock - providing promising conditions for efficient stochastic acceleration** (Virtanen & Vainio 2005)

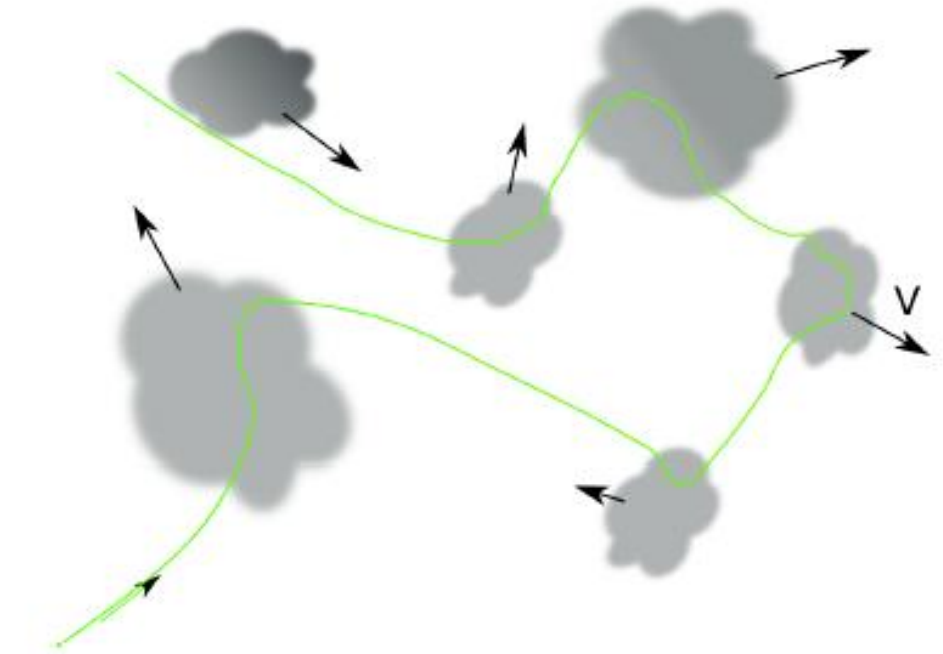

$$\frac{\Delta\varepsilon}{\varepsilon} \propto \left(\frac{V}{c}\right)^2$$

- **Relativistic shocks In BL Lac jets: turbulent structures can be strongly amplified in shocked material** (Marcher 2014, Mizuno+2014)
- **Stochastic process: not tied to the plasma speed ➔ Continue particle accelerate far away from the shock and for much longer than the first-order process – provided the sufficient turbulence present** (Tammi & Duffy 2009)

- Tramacere +2011: **Log-parabolic particle energy distribution represents the general solution of the energy- and time-dependent Fokker–Planck equation that includes systematic (e.g. BZ-mechanism) and stochastic (momentum diffusion due to resonant interactions with turbulent MHD modes) accelerations together with radiative/adiabatic cooling as well as particle escape and injection terms**

$$\frac{\partial n(\gamma,t)}{\partial t} = \frac{\partial}{\partial \gamma}\left\{ -[S(\gamma,t) + D_A(\gamma,t)]n(\gamma,t) + D_p(\gamma,t)\frac{\partial n(\gamma,t)}{\partial \gamma}\right\} - \frac{n(\gamma,t)}{T_{\rm esc}(\gamma)} + Q(\gamma,t),$$

extra-term describing systematic energy loss *and/or gain*

average energy change term due to the momentum-diffusion process

momentum-diffusion coefficient

escape term

injection term

- **Neglecting S and T_{esc}, using a mono-energetic and instantaneous injection ($n(\gamma,0)=N_0\delta(\gamma-\gamma_0)$, the solution is** (Tramacere+2011)

$$n(\gamma,t)=\frac{N_0}{\gamma\sqrt{4\pi D_{p0}t}}\exp\left\{-\frac{[\ln(\gamma/\gamma_0)-(A_{p0}-D_{p0})t]^2}{4D_{p0}t}\right\},$$

i.e., a log-parabolic distribution with the curvature term

$$r=\frac{c_e}{4D_{p0}t}\propto\frac{1}{D_{p0}t}.$$

- **Synchrotron SED expected to be** (Massaro+ 2011)
  - **relatively broader (i.e., lower curvature, *b* ~ 0.3) when the efficient stochastic acceleration (expected in TeV-detected HBLs)**
  - **narrower (*b* ~ 0.7): less-efficient stochastic acceleration (TeV-undetected HBLs)**

- **0.3-10 keV spectra of Mrk 421 during 2005-2018 (Swift-XRT observations): >90% of *b* values with *b* ~0.3 or smaller** (Kapanadze+2016a, 2017, 2018a,b, 2019)

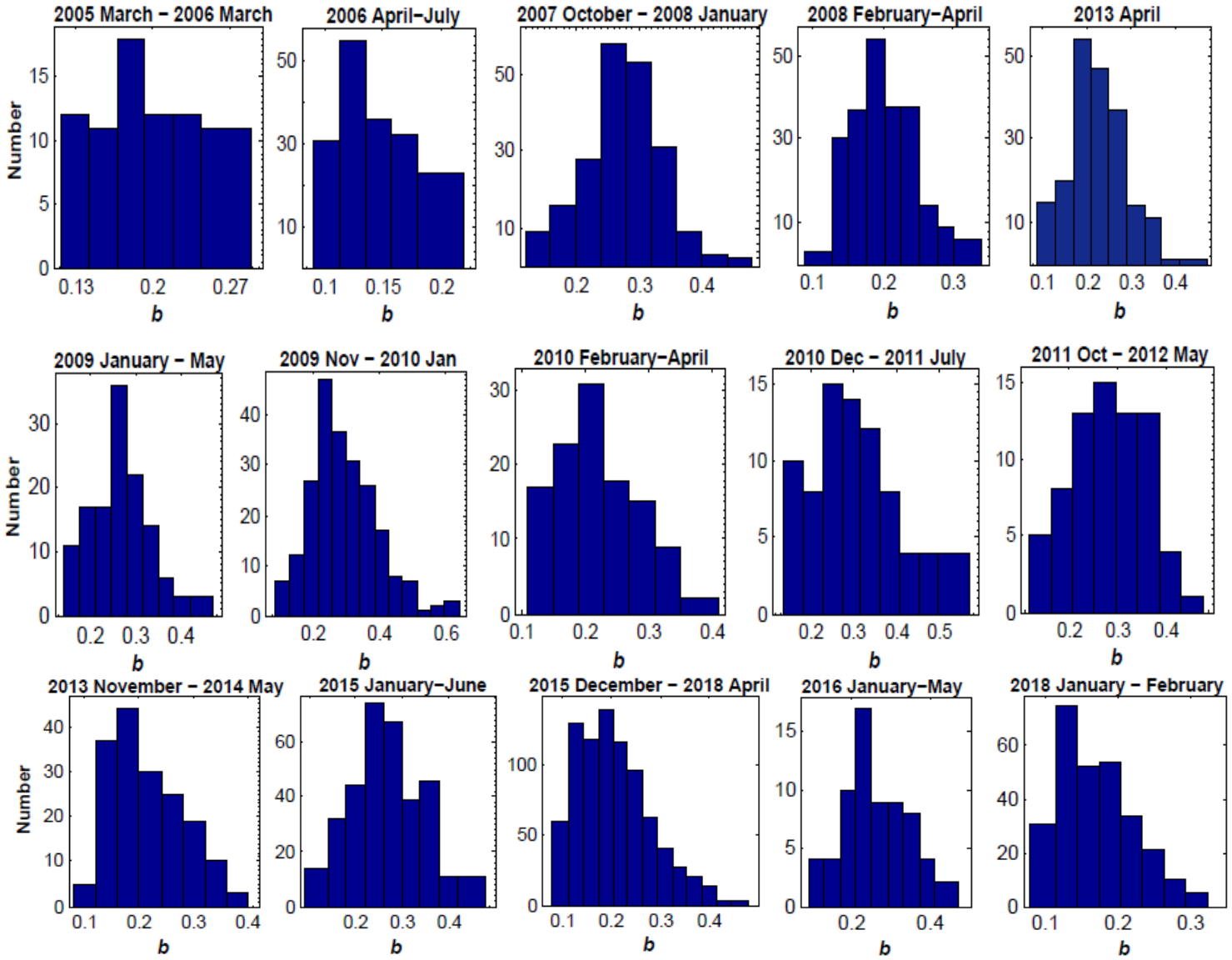

- $E_p - b$ **anticorrelation, predicted for stochastic acceleration** (Tramacere+2011): **observed in different periods, although *weak* or very *weak*** (Kapanadze+2016a, 2017, 2018a,b, 2019)

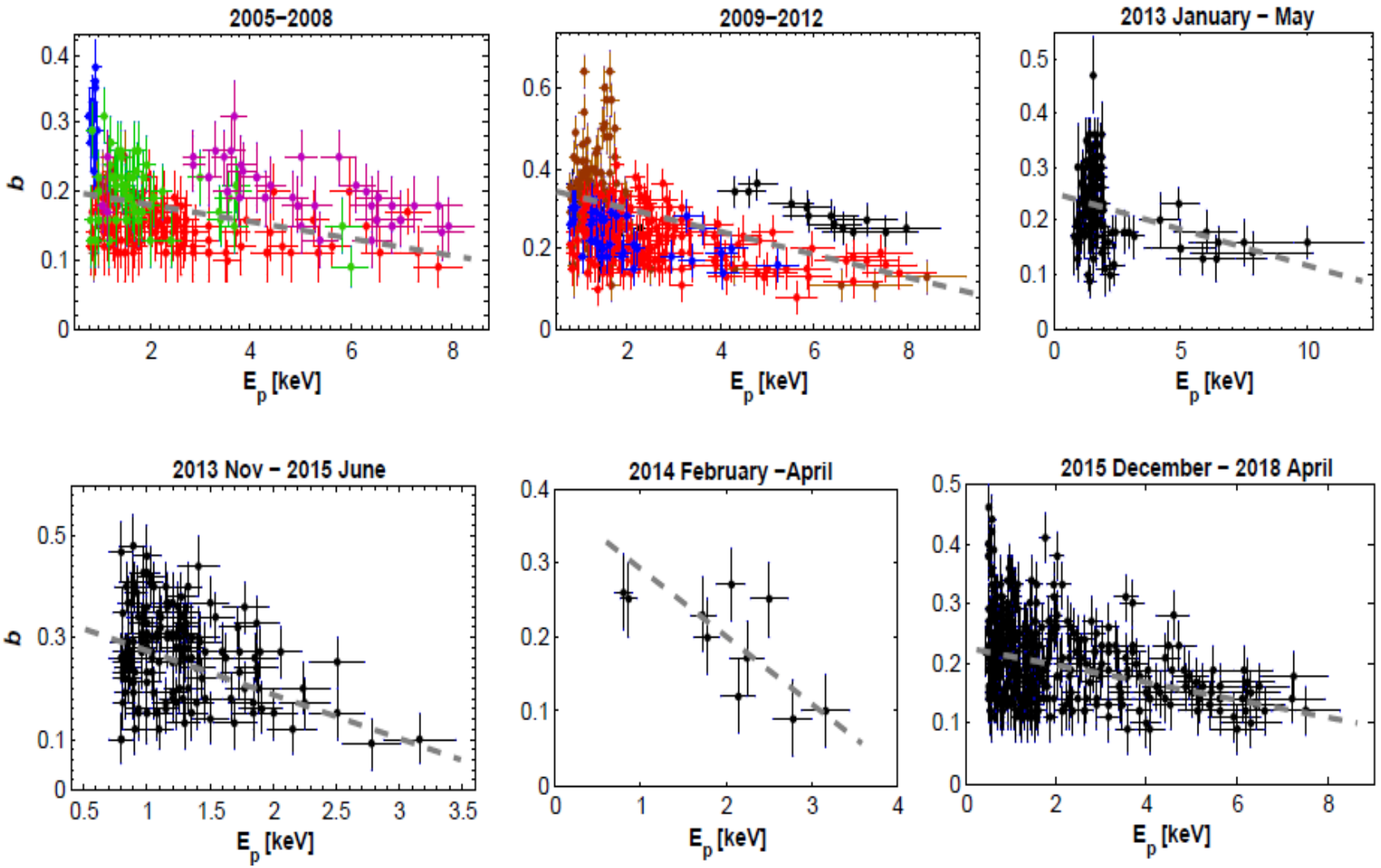

Correlation weakness - possible reasons:

- **we have not included the spectra with E_p <0.5 keV in our study - the synchrotron SED peak is poorly constrained by Swift-XRT data ➔ the E_p value obtained with X-ray spectral analysis (XSPEC package) to be considered as upper limit to the intrinsic position**
- **EDAP also implies the $E_p - b$ anticorrelation, although with different slope in the scatter plot: log E_p ~3/(10b) versus log E_p ~1/(2b) for stochastic process** (Chen 2015)
- **competing acceleration and cooling processes, not yielding the logparabolic distributions:**
  - **"classical" first-order Fermi acceleration, reconnection, shear acceleration – establishing powerlaw distributions and diminishing the observed curvature (possibly, the case for the spectra with b$\lesssim$0.2)**

- **Detection of the correlation $S_p \propto E_p^{\alpha}$ (S_p - SED peak height): discern the physical factor making the main contribution to the observed spectral variability depending on the values of the exponent α** (Tramacere+2011):
  - ***α =0.6*** **- the parameters *D_p (momentum-diffusion coefficient) and q* (the exponent describing the turbulence spectrum) variable during the stochastic acceleration process: transition from the Kraichnan (*q = 3/2*) into "hard sphere" spectrum (*q = 2*)**
  - ***α=1 – 4 :*** **changes in the number and energy of emitting particles, magnetic field, beaming factor)**
- **Our study: the presence of the $S_p \propto E_p^{\alpha}$ relation with $\alpha \sim 0.6$ in some epochs of the efficient stochastic acceleration in Mrk 421 (**Kapanadze+2018a, 2019)

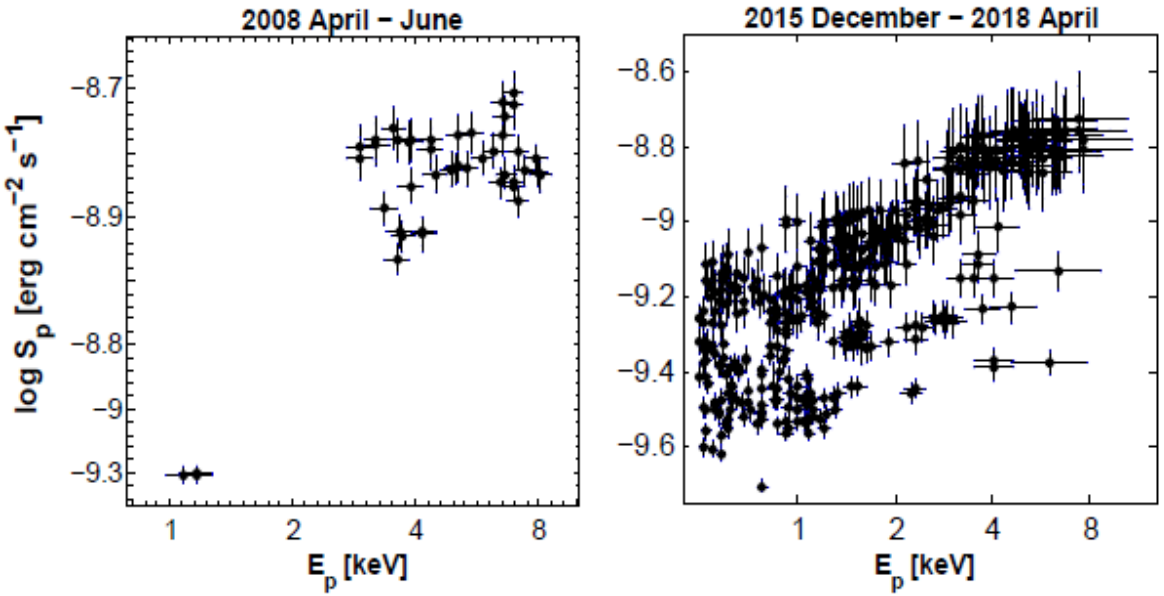

- **Other periods: *$\alpha \sim 0.3–0.4$***
  - **no clearly-expressed dominant factor**
  - **assumption about the synchrotron emission from one dominant homogeneous component - inappropriate for Mrk 421**

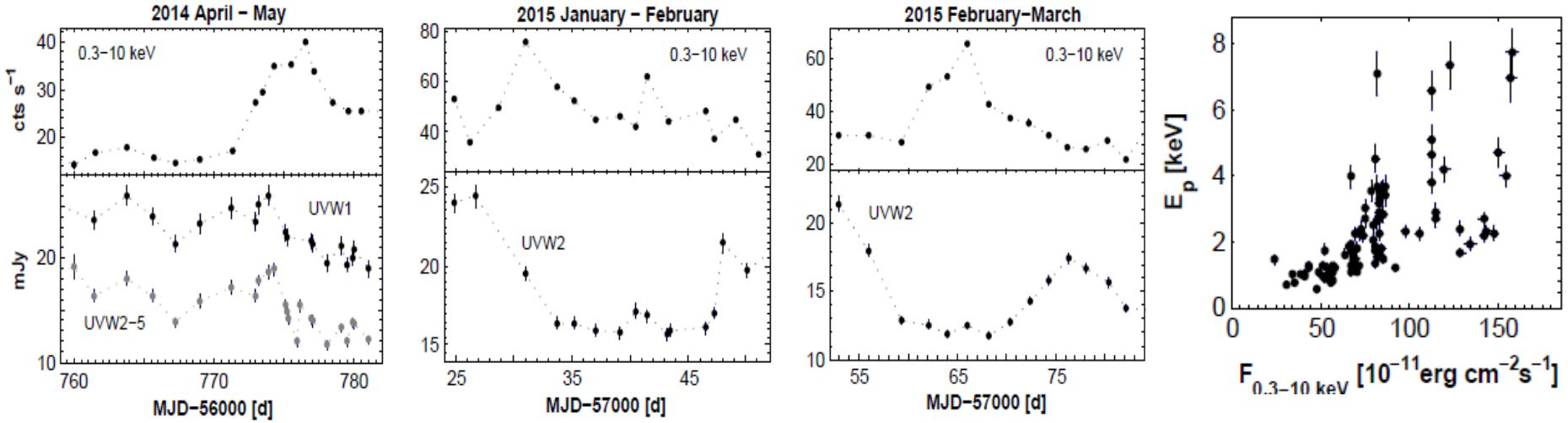

- **Frequent occurrence of declining optical-UV brightness in the epochs of X-ray flares** (Aleksic +2015; Kapanadze+2016,2017,2018a,b, 2019)

- **Explanation: hardening in the electron energy distribution, shifting the entire synchrotron bump to higher energies, leading to a brightness decline at lower frequencies while the X-ray brightness is rising** (Aleksic +2015) ➔ **Corroborated by our finding of a positive E_p–$F_{0.3\text{-}10\ keV}$ correlation ➔ Shift of the synchrotron SED peak toward higher energies with increasing X-ray flux**

- **Underlying physical mechanism:** ***stochastic acceleration of electrons with narrow initial energy distribution, having an average energy significantly higher than the equilibrium energy*** (Katarzynski+2006)

The acceleration time-scale for stochastic acceleration is (Rieger, Bosch-Ramon & Duffy 2007)

$$\tau_{\rm FII} \approx \frac{3}{4}\left(\frac{c}{v_{\rm A}}\right)^2 \frac{\lambda}{c} \approx \frac{3}{4}\frac{c r_{\rm g}}{v_{\rm A}^2}, \qquad (4)$$

where the Alfvén speed, defined by

$$v_{\rm A}^2 = \frac{(B\,c)^2}{4\pi h n + B^2}, \qquad (5)$$

depends on the enthalpy, $h = (\rho + P)/n$, with the energy density of the plasma, $\rho = nmc^2$, being a function of the composition and number density, n. The mass m depends on the composition and is $m_{\rm ee} = 2m_{\rm e}$ for pure electron–positron plasma, and $m_{\rm ep} = m_{\rm e} + m_{\rm p}$ for ionized hydrogen. The effect of the gas pressure, P, is taken to be negligible.

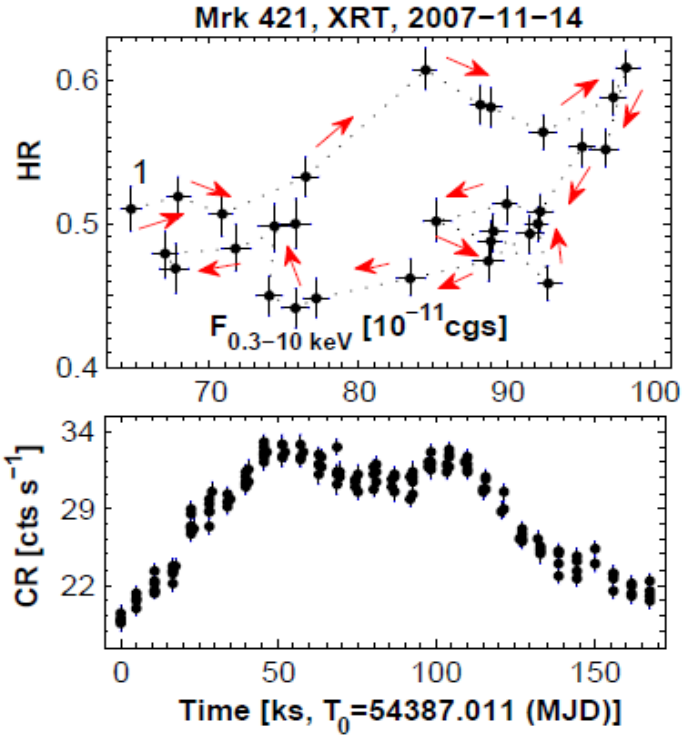

- **Stochastic acceleration: very slow for**
  - **relatively low magnetic field**
  - **high matter density**

- **Counter-clockwise (CCW) spectral evolution in the hardness ratio – flux plane in the case of gradual acceleration** (Cui 2004)

- **Stochastic mechanism: gradual acceleration of particles versus the fast injection expected within first-order Fermi process** (Tammi & Duffy 2009)

- **Transition from the log-parabolic into a power-law spectrum and vice versa, within 1 ks observational run (frequently detected within our study) ➔ Extremely rapid changes of the magnetic field properties in the emission zone: from the state with a decreasing confinement efficiency with increasing gyro-radius (or from the turbulent state, both yielding a log-parabolic spectrum) into that without these properties (power-law spectrum), and vice versa**

- **Frequently observed case for bright HBLs: CCW-loop during some longer-term X-ray flares, although including a CW sub-loop corresponding to the shorter-term, lower amplitude flare superimposed on the long-term variability trend: passage of the shock through jet area with different physical conditions? (e.g. standing shock generated due to different jet instabilities)**

- **Opposite cases also frequently observed**

Relativistic Magnetic Reconnection

- **Driven mostly by kink instability**
- **Efficient convertor of magnetic energy into bulk motion, heat, energetic particles**
  - **cold, magnetized plasma enters the reconnection region**
  - **plasma leaves the reconnection region at the Alfvén speed $\sim(1+\sigma)^{1/2}$**
  - **transfers ~ 50% of the flow energy (electron-positron plasmas) or ~ 25% (electron-proton) to the emitting particles**
- **expected to operate effectively in the highly-magnetized jet areas ($\sigma>>1$)**
- **"Relativistic" regime in astrophysical jets: magnetic energy per particle exceeding rest mass energy** (Sironi & Spitkowsky 2014)
- **Dissipation distance from SMBH: from $\sim 100 r_g$ up to several hundreds pc, with the peak rate at a few pc** (Giannios & Uzdensky 2019)
- **Providing a promising explanation for the long-wavelength (radio-to-optical) flares:**
  - ❑ **For $\sigma \gtrsim 10$, the particle spectrum is hard (power-law slope $p<2$) and tends to asymptote to $p = 2$ (for the energies $\gamma<10^2$ - sufficient to produce only synchrotron radio photons) at earlier acceleration stages; the steepening of the power-law slope allows the spectral cutoff to extend to higher and higher energies**

• **However, fewer expected contribution to the keV-TeV part of the broadband SED of Mrk 421 (compared to the other acceleration mechanisms):**

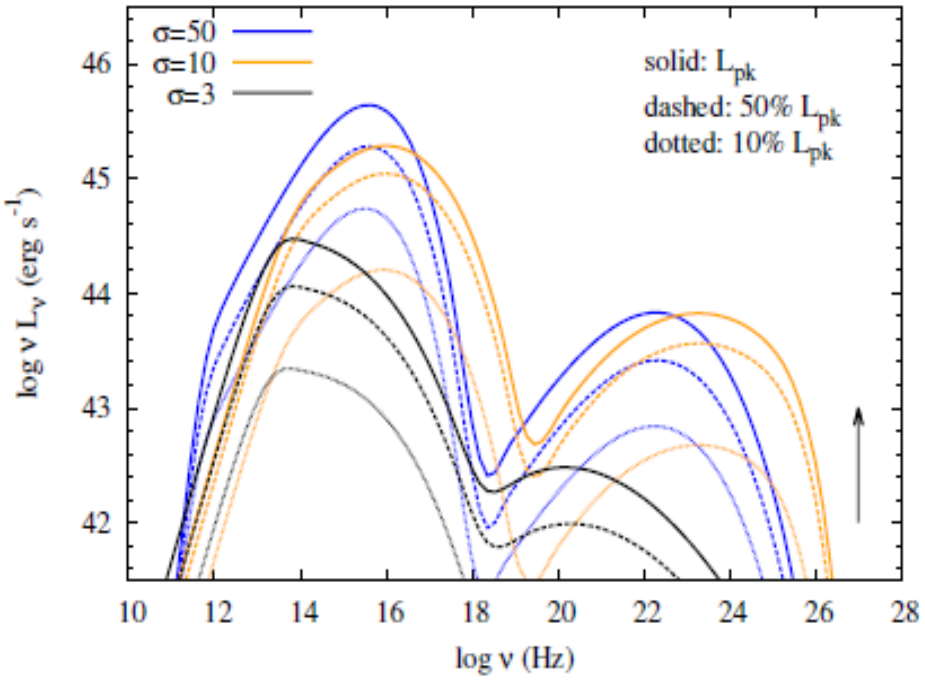

Figure 12. Comparison of the multi-wavelength photon spectra obtained during the growth phase of a small and relativistic plasmoid for the three magnetizations considered in this study. The snapshots of the photon spectra correspond to the peak time of the flare (solid lines) and to times where the bolometric luminosity is at 10% (dotted lines) and 50% (dashed lines) of its peak value. The arrow shows the time flow.

(Petropoulou+2016, MNRAS, 462, 3325)

- **large number of electrons with $\gamma \sim 10^5$-10^6 are required to produce X-ray (synchrotron mechanism) and gamma-ray (IC in the Thosmon regime) photons**
- **several days to a few weeks are necessary to accelerate electrons to these energies: at later stages of the reconnection acceleration, the spectral cutoff scales with the acceleration time as $\gamma_{cut} \sim \sqrt{t}$, plus the additional boost by a factor of m_p/m_e in the electron-proton plasma, although very high magnetization needed ($\sigma \gtrsim 1000$; Nalewajko 2018)**

Shear acceleration

- **Fermi acceleration without a shock - wherever scattering centres flow at different speeds, even if the flows are parallel (e.g. ,longitudinal shear across the jet radius) - particles intercepted by the difference between the fast core of the jet and the slower exterior** (Rieger & Duffy 2016)
- **accelerates particles slowly compared to other hypothetic mechanisms and can not be important for very fast X-ray – TeV flares** (Tammi & Duffy 2009)
- **Rieger & Duffy 2016**: **shear acceleration can overcome radiative and non-radiative losses and work efficiently, when the pre-accelerated seed particles are available - continue to accelerate the particles already energized by the first- or second-order mechanisms and can be important for longer-term variability (poorly studied case - our future "target"!)**
- **The inverse dependence on the particle mean free path makes shear acceleration a preferred mechanism for accelerating hadrons** (Rieger & Duffy 2016): **our future "target"!**

Jet-star interaction

- **The winds of stars (bubbles from red giants) interacting with AGN jets produce a double bow-shock structure in which particles can be accelerated to relativistic energies, possibly contributing to the jet's total non-thermal emission** (Torres-Alba & Bosh-Ramon 2019)

- **The predicted apparent luminosities of the IC emission: a few times 10^{40} erg/s – much smaller than the low-state LAT-band or VHE luminosity of Mrk 421**

- **Unlike in the case of the IC emission, synchrotron emission can be 1–3 orders of magnitude higher for strong magnetic field and its peak value comparable to the IC emission of Mrk 421, produced by other mechanisms, at E~100 keV (and even at higher energies within some favourable conditions**; N. Torres-Alba, private communication**)**

$L_{\rm j}$ [erg s^{-1}]	10^{43}	10^{44}	10^{45}	10^{43}	10^{44}	10^{45}
Γ	3	3	3	10	10	10
Inverse Compton: $E'_{\rm e} = E'_{\rm IC}$ $B = 0.1B_{\rm eq}$						
$L_{\rm st}$ [erg s^{-1}]	6.5×10^{39}	1.7×10^{40}	1.7×10^{40}	2.5×10^{39}	6.9×10^{39}	1.8×10^{40}
$L_{\rm pop}$ [erg s^{-1}]	1.1×10^{38}	6.5×10^{38}	8.4×10^{38}	3.7×10^{40}	4.7×10^{40}	3.4×10^{40}
Synchrotron: $E'_{\rm e} = E'_{\rm Sy}$, $B = B_{\rm eq}$						
$L_{\rm st}$ [erg s^{-1}]	7.5×10^{41}	1.9×10^{42}	1.9×10^{42}	1.3×10^{41}	7.4×10^{41}	2.5×10^{42}
$L_{\rm pop}$ [erg s^{-1}]	1.4×10^{40}	4.0×10^{40}	6.7×10^{40}	1.1×10^{42}	2.0×10^{42}	2.5×10^{42}
$L_{\rm peak}$ [erg s^{-1}]	5.8×10^{41}	5.8×10^{42}	5.8×10^{43}	6.3×10^{42}	6.3×10^{43}	6.4×10^{44}

- **Frequent occurrence of soft γ-ray excess at the energies below 2 GeV during the Fermi-LAT observations of Mek 421 during 2016 April November (Kapanadze+2019) - contribution from the synchrotron photons from ultra-relativistic leptons accelerated to the jet-star interaction?**

- **Our study is performed for the energy range 300 MeV – 300 GeV (general case for HBLs)– to be extended to the range of 100-300 MeV and earlier time intervals.**

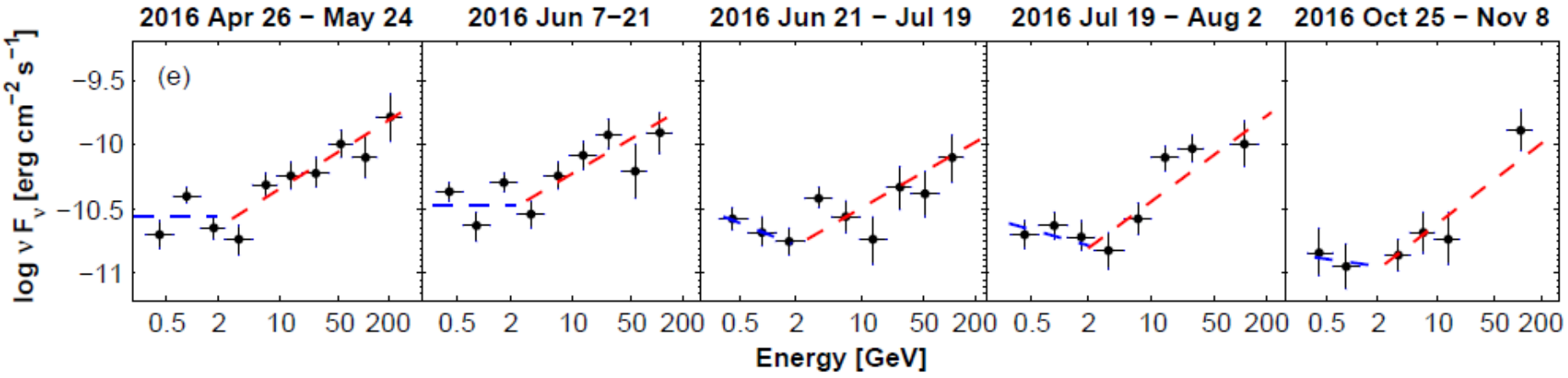

Summary and Conclusions

- **Mrk 421 – one of the most extreme particle accelerators in the universe**
- **The closest and brightest BL Lacertae source - an unique opportunity to perform a detailed study the blazar nature, where the acceleration and radiative evolution of freshly accelerated particles can be tracked**

- **Most plausible acceleration mechanisms:**
  - **BZ-mechanism: jet launching and acceleration of the particles up to ultra-relativistic energies within the hundred Swarzschild radii**
  - **Additional acceleration processes needed for generating X-ray and gamma-ray emissions on sub-pc, pc and even on kpc scales, explaining the timing and spectral signatures:**
    - **first and second order Fermi mechanisms, related to the propagation of relativistic shocks and turbulent structures in the jets**
    - **possible "competition" between different acceleration mechanisms ("classical" first-order Fermi acceleration yielding a powerlaw energy spectrum, EDAP, stochastic acceleration etc.) resulting in a weakness or even absence of both $E_p - b$ and a-b correlations, expected for the Fermi mechanisms**

- Observation of the correlation $S_p \propto E_p^{\alpha}$ with $\alpha \sim 0.6$ in some periods, implying a change in the turbulence spectrum in the jet area producing X-ray emission
- Stochastic acceleration in the jet areas with different matter density, composition and magnetic field may yield as instantaneous, as gradual acceleration of the electrons to the energies necessary for producing X-ray photons, resulted in both CW an CCW loops in HR-flux plane
- Optical-UV decline along with X-ray flares, explained by stochastic acceleration of electrons with a narrow initial energy distribution, having an average energy significantly higher than the equilibrium energy
- Possible importance of relativistic magnetic reconnection to accelerate particles to the energies allowing to produce radio-optical photons and then upscatter to MeV-GeV energies
- Possible contribution of star-jet interaction to the soft gamma-ray emission during 2016 April-November

Thanks for

- your attention
- Dr. Josep Paredes, for the invitation

The presentation was supported by Shota Rustaveli National Science Foundation of Georgia (SRNSFG) [grant number MG-TG-19-360]